ANALYSIS OF THE EFFECTS CAUSED BY PARAMETER INHOMOGENEITY WITH A 2D MODELLING TOOL BASED ON CIRCUIT SIMULATION

M. Köber[1], M. Hermle[1], J. Isenberg[1*], M. Kasemann[2], H. Cárdenes[3], W. Warta[1]
[1] Fraunhofer Institute for Solar Energy Systems ISE, Heidenhofstr. 2, 79110 Freiburg, Germany
[2] Freiburger Materialforschungszentrum, Stefan-Meier-Str. 21, 79104 Freiburg, Germany
[3] Langobardenstr. 3, 70435 Stuttgart, Germany, * present address: Q-Cells, 06766 Thalheim, Germany
phone: +49 761 45885201, fax: +49 761 45889250, email: mariana.koeber@ise.fraunhofer.de

ABSTRACT: In silicon solar cells many parameters may be laterally inhomogeneous, e.g. R_s, R_p and lifetime. In recent years powerful tools for imaging inhomogeneous properties have been established. Examples of measurements show that the potential distribution is a key parameter. A circuit simulation program with input options for several inhomogeneous parameter sets was developed in the European project PORTRAIT. The program is introduced and applications are demonstrated on example situations of parameter inhomogeneities: the potential distribution caused by a severe shunt, the impact of regions of low lifetime beneath the front metallisation, different lifetime distributions for a n-type solar cell with rear side emitter, the impact on the *IV* parameters when the two parameters lifetime and parallel resistance are inhomogeneous and the fill factor loss caused by finger interruptions. Excellent agreement of the simulated potential distribution resulting from strong shunts with V_{oc}-PL measurements is demonstrated. The experimental observation that higher efficiencies are reached if impurities are concentrated locally instead of widely spread is confirmed. For finger interruptions a strong position dependence of these interruptions was observed.
Keywords: simulation, parameter inhomogeneity, crystalline silicon

1 INTRODUCTION

Industrial silicon solar cells frequently exhibit strong lateral inhomogeneities in the parameters lifetime, R_s and R_p, amongst others. Spatially resolved measurement techniques (e.g. SR-LBIC, CDI [1] / ILM [2], ILIT [3], EL [4], PL [5],...) have become state of the art tools for assessing material and process quality in silicon solar cells. An example of a cell with strongly inhomogeneous parallel resistance, measured with V_{oc}-ILIT (Illuminated Lock-In-Thermography) as well as V_{oc}-PL (Photoluminescence) is shown in Fig. 1. While ILIT displays the local losses by their thermal effects, PL images the inhomogeneity of the potential across the pn-junction caused in this case by the shunts. In addition, in both cases recombination losses by low lifetime regions are visible. Note that the PL signal, since it is proportional to carrier density, is exponentially related to the local potential [6].

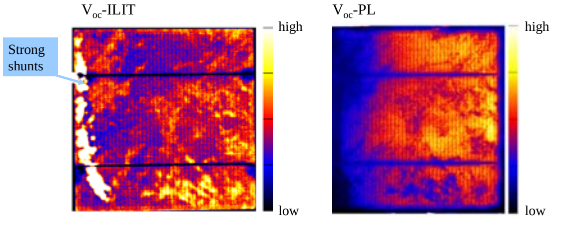

Fig. 1: Example of inhomogeneous parallel resistance, measured with V_{oc}-ILIT (left, power loss visualised by a thermal image) as well as V_{oc}-PL (right, potential drop visualised by the carrier density).

Although global parameters may often be obtained by appropriate averaging [7], the quantitative impact of imaged inhomogeneities especially of more than one parameter on cell performance is mostly unclear. As an important step to solve this problem the easy-to-handle circuit simulation software PORTRAIT was developed.

The simulation principles are outlined and the capabilities demonstrated by a first set of example calculations aiming at an understanding of the effects caused by the interactions of several inhomogeneous factors.

2 THE SIMULATION SOFTWARE

The correct description of the cell performance solving the semiconductor equations in three dimensions is impractical. A circuit simulation allowing the consideration of most parameters of interest in a reasonable time-frame was developed during the EU-project PORTRAIT. It is based on the circuit simulation tool CIRCUS [8]. The PORTRAIT simulation tool is easy to handle and platform-independent.

2.1 Principle of the circuit simulation

The solar cell is subdivided into n x n nodes. For each elementary diode the local *IV* curve is calculated. The nodes are interconnected by a resistance network solving Kirchhoffs laws for every node in the circuit.
Fig. 2 shows a scheme of the circuit model. Only currents in the emitter as well as the front and rear metallisation are considered. Lateral currents in the basis have to be negligible. This holds true for lifetime matrices with structure size W_τ > effective diffusion length L_{eff} [7]. For a definition of W_τ see Fig. 8.

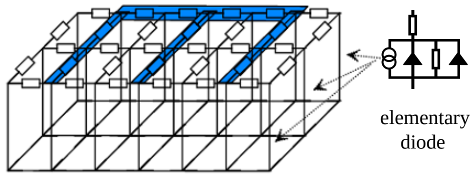

Fig. 2: Resistance network and elementary diode of the solar cell model used in the PORTRAIT circuit simulation.

2.2 PORTRAIT simulation

The local illuminated and dark *IV* curves for a specific cell technology are simulated using PC1D [9]. In the actual version the parameters that can be varied are R_s, R_p and one further parameter that is varied in PC1D (e.g. lifetime, I_{02}, S_{rear}, cell thickness...). The injection dependence of the lifetime can be considered by including it in the PC1D model. The output of the calculation consists in the global *IV* curve, the *IV* parameters and matrices of voltage, current and power at V_{oc}, the maximum power point and J_{sc}. This allows the illustration of voltage drops and thus insight into physical processes in the cell.

3 EFFECTS OF PARAMETER INHOMOGENEITY

First examples of the use of the PORTRAIT simulation tool to model potential drops and to obtain quantitative statements of the impact of inhomogeneities on solar cell parameters are given. In section 3.1 the potential drop caused by strong shunts is simulated for a comparison to the V_{oc}-PL in Fig. 1. In section 3.2 the effect of regions of low lifetime beneath the front metallisation on the *IV* parameters is studied, in section 3.3 inhomogeneities in lifetime in an n-type solar cell with rear side emitter are analysed. The interaction of simultaneous inhomogeneity in R_p and lifetime is considered in section 3.4. Finally, in section 3.5 the fill factor loss caused by finger interruptions at different positions of the cell surface is studied.

3.1 Potential drop caused by strong shunts

In order to understand the distribution of the carrier density measured with V_{oc}-PL for a cell with strong shunts (Fig. 1), the potential drop caused by these shunts, shielded by serial resistances, was simulated. The geometry of the shunts was taken from the V_{oc}-ILIT measurement (Fig. 1), the strength of the shunt was set such that the normalised R_p-value gave the global R_p-value extracted from the fit of the 2-diode model to the dark *IV* curve. Furthermore, the R_s-matrix was modelled including measured values for the contact, metallisation and emitter sheet resistances. For simplicity, lifetime was assumed to be homogeneous. Since V_{oc}-PL is measuring the carrier density which scales exponentially with the potential, in Fig. 3 (left) exp(V/kT) is plotted.

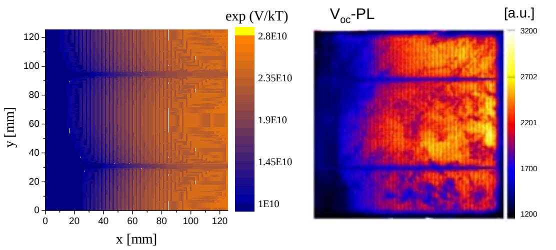

Fig. 3 left: exp(V/kT) calculated for the cell from Fig. 1; right: V_{oc}-PL shown in Fig. 1.

Comparing the outcome of the calculation with the V_{oc}-PL image, one finds excellent agreement. The impact of these strong shunts on the low carrier density observed in the V_{oc}-PL image is reproduced in the calculation.

3.2 Low lifetime beneath front metallisation

Observations from V_{oc}-ILIT measurements in combination with lifetime measurements led to the conclusion that regions of low lifetime beneath the front metallisation can act like a shunt [10]. At the maximum power point only a weak correlation of recombination signal and thermal signal was observed, and no correlation at I_{sc}.

To assess the effect of the position of regions of low lifetime in relation to the front metallisation on the *IV* parameters a cell with typical industrial technology was simulated. The following inhomogeneities in lifetime were considered: (i) simplified multi-crystalline material with different grain sizes as shown in Fig. 4, (ii) regions of low lifetime that are restricted to 5 % of the cell surface and (iii) regions of low lifetime collocated lamellar as in EFG material. A variation of the lifetime values as well as of the emitter sheet resistance was performed, whereby S_{front} was left fix for reasons of comparability (thus the simulated cell with high sheet resistivity is not really a high efficiency cell).

For the lifetime distribution depicted in Fig. 4 the two situations in which the low lifetime regions are either always beneath the metallisation fingers or between the fingers were compared. Note that this is possible only for very small lifetime structures (e.g. grain boundaries).

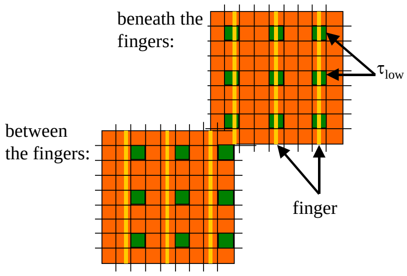

Fig. 4: Lifetime configuration simulating multi-crystalline material. The regions of low lifetime are either always beneath or between the fingers.

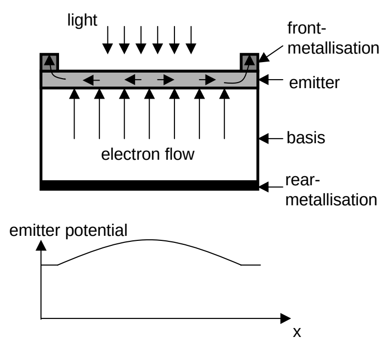

Fig. 5: Electron flow and emitter potential in an illuminated n^+p-solar cell under J_{sc} conditions [10].

For the lifetime configuration with low lifetime beneath the fingers the expected loss in V_{oc} was significant only if τ_{low} assumed low values (τ_{high} = 50 µs, τ_{low} = 0.1 µs). Interestingly, for this case a marked increase in *FF* was observed.

An explanation for this difference in *FF* may be the recombination current. The recombination current depends exponentially on the potential. At the maximum power point at which current is flowing the emitter potential is lower beneath the metallisation fingers than in between the fingers (see Fig. 5). This results in a lower recombination current if the regions of low lifetime are beneath the fingers.

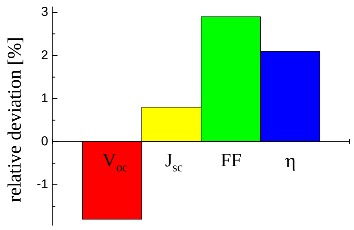

Fig. 6: Relative difference in solar cell parameters for the two lifetime configurations shown in Fig. 4 and a 40 Ω/Square emitter.

As a consequence and quite contrary to expectations, efficiency is higher if the regions of low lifetime are beneath the grid. The results for a 40 Ω/Square emitter are depicted in Fig. 6. The effect increases significantly with increasing emitter sheet resistance (see Fig. 7).

If the regions of low lifetime are restricted to a small percentage of the cell (5 %) no significant differences in *IV* parameters resulted from different position relative to the metallisation.

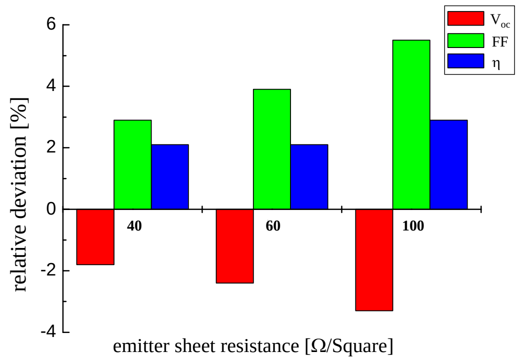

Fig. 7: *IV* parameters for lifetime distribution from Fig. 4 for variable emitter sheet resistance.

In order to estimate maximum effects for EFG material regular lifetime stripes were simulated, lying either beneath, in between or orthogonal to the fingers. For lifetime values of τ_{high} = 50 µs and τ_{low} = 0.1 µs and an emitter sheet resistance of 100 Ω/Square a strong effect was found (6.7 % relative on efficiency). However, a calculation with a first example of lifetime extracted from an SR-LBIC measurement resulted in no significant difference for arranging the lifetime stripes parallel or orthogonal to the fingers. τ_{low} was 5-10 µs in this case.

3.3 Inhomogeneous lifetime for an n-type solar cell with rear side emitter

For an n-type solar cell with rear side emitter (see Fig. 8, left) the impact of different grain size of multi-crystalline material for equal average diffusion length was analysed. A "chess board"-type lifetime matrix was simulated (Fig. 8, right), the structure size W_τ and the n^{++}- sheet resistance were varied.

For different structure size differences result only in V_{oc}. They are significant (> 1 % relative) only if the smaller lifetime is fairly low (τ_{low} = 1 µs, τ_{high} = 1000 µs) and the n^{++}-layer highly resistive (120 Ω/Square) as shown in Fig. 9. With such low lifetimes efficiency is already influenced strongly.

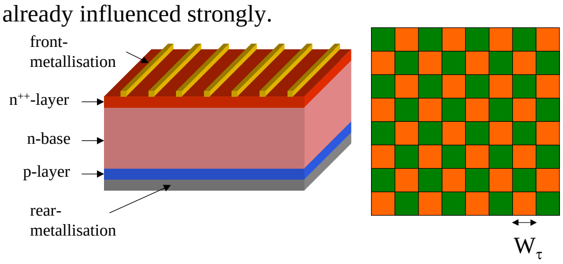

Fig. 8: Schematic of the simulated n-type cell with rear side emitter (left) and lifetime configuration "chess board" with structure size W_τ (right).

One important consequence of this study is that higher efficiencies are reached if impurities are concentrated at one spot instead of widely spread with less density, or for multi-crystalline material with big grain size than small grain size (for equal average lifetime). This was already found experimentally [11].

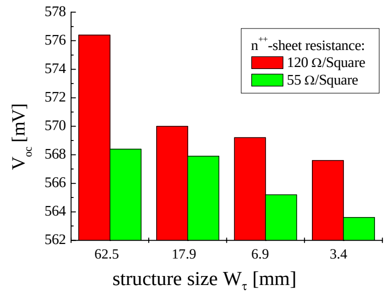

Fig. 9: V_{oc} for the n-type solar cell with rear side emitter and lifetime distribution with structure size W_τ as depicted in Fig. 8, for two different emitter resistivities.

3.4 Ohmic shunt in regions of different material quality

The impact of the shunt position with respect to grains with different quality in multi-crystalline material was studied. Again, an industrial cell was modelled.

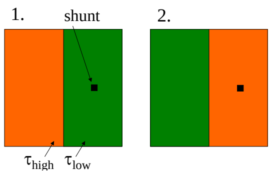

Fig. 10: Arrangement of a shunt in a region of low lifetime (1.) and high lifetime (2.).

The solar cell was divided into two regions of low and high lifetime (τ_{low} = 1 µs, τ_{high} = 100 µs). A shunt was situated once in the low lifetime region, once in the high lifetime region, as shown in Fig. 10. Because of the strong correlation of R_s with R_p the shunt position was held fix with respect to the metallisation grid. The lifetime matrix was "switched". An injection dependence of the lifetime was accounted for resembling a Fe-impurity. The strength of the shunt was varied. Contrary to prior expectations, neither in *FF* nor in V_{oc} a significant difference was found (see Fig. 11).

The present understanding of this result is that the fill factor is dominated completely by the ohmic shunt for the parameter configuration chosen. For weak ohmic shunts the open circuit voltage is not influenced by the shunt. When the shunt is starting to influence V_{oc}, the potential difference caused by the different splitting of the Fermi-level for the two different lifetime regions is small compared to the potential difference caused by the shunt, leading to negligible difference in V_{oc}.

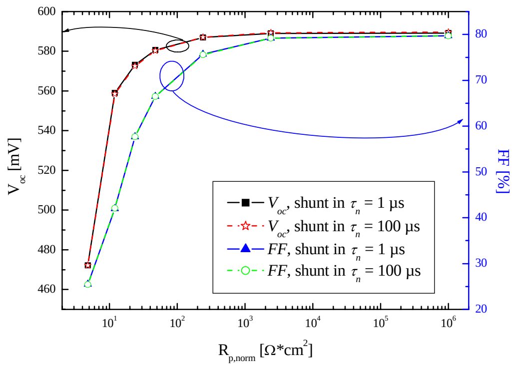

Fig. 11: Open circuit voltage and fill factor versus normalised parallel resistance for the two cases shunt situated in the region of high or low lifetime.

3.5 Fill factor loss caused by a finger interruption

Finger interruptions occur in screen-printed metallisation due to failures in the process (e.g. clogging of the screen). The Portrait simulation tool enabled us to assess the impact of finger interruptions on the global *IV* curve quantitatively. However, because of a strong increase in calculation time with an increase in the number of nodal points, at present one is restricted in choosing the length of the finger interruption. In the following example the length of the finger interruption was chosen to be 870 µm. The position dependence of the fill factor loss caused by a finger interruption was analysed.

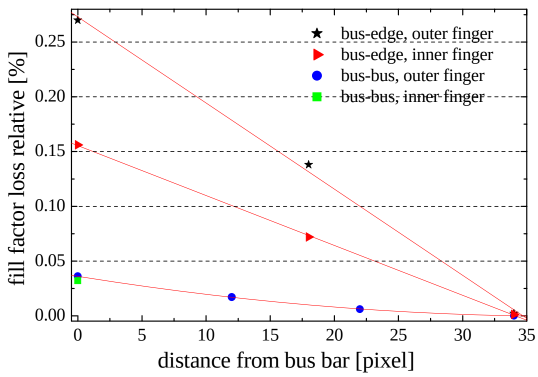

Fig. 12: Relative fill factor loss versus distance of the finger interruption from the bus bar for the four types of fingers to be distinguished (see text).

A first analysis leads to the necessity of the distinction of inner fingers (which have two neighbour-fingers) from outer fingers (only one neighbour-finger) as well as the bus-bus region (fingers that connect two bus bars) from the bus-edge region (fingers that lead from the cell edge to a bus bar). For these fingers the dependence of the fill factor loss from the distance to the bus bar was studied. The type of dependence was first determined on smaller cell sections, in order to minimise calculation time. A linear dependence was found for the region bus-edge, a quadratic dependence for the region bus-bus. The values calculated for the full cell are given in Fig. 12.

A strong position dependence was found. Especially interruptions of fingers that lead from the cell edge to a bus bar reduce the fill factor. A redundant line would diminish the damage caused by an interruption on these fingers.

If finger interruptions are assumed to be statistically distributed (equal probability for all positions), the mean *FF*-loss is $\Delta FF_{mean} = 0.05\,\%$ per interruption. n finger interruptions scale linear ($n*\Delta FF$).

4 CONCLUSIONS

The Portrait circuit simulation program is ready for application to the widely unclear effects of interaction of different parameter inhomogeneities in industrial cells. It is platform-independent and easy to handle. A first set of calculation examples demonstrates its capabilities. Physical insight could be gained on the impact of the potential distribution between fingers on recombination activity of local defects in dependence of the emitter sheet resistance. For finger interruptions a strong position dependence was found. The present study serves as a starting point, results so far are likely to depend on details of the specific parameter sets chosen. Potential impact on understanding of production cells is high, but in order to achieve decisive statements more elaborate tests are needed. To ease them an improvement of the calculation speed (at present still many hours for a useful node density of e.g. 140x140) is envisaged.

ACKNOWLEDGEMENTS

The authors would like to thank O. Breitenstein for his co-operation. This work has been supported by the EC under contract ENK6-CT2001-00573 (PORTRAIT) and by the German BMBF in the “Netz Diagnostik”.

REFERENCES

[1] S. Riepe et al., Proc. 17th EC-PVSEC, Munich, 2001, p. 1597
[2] M. Bail et al., Proc. 28th IEEE-PVSC, Anchorage, 2000, p. 99
[3] J. Isenberg, A.S.H.v.d. Heide and W. Warta, Proc. 20th EC-PVSEC, Barcelona, 2005, p. 136
[4] T. Fujuki et al., Appl. Phys. Lett. **86**, 262108 (2005)
[5] T. Trupke et al., *FAST PHOTOLUMINESCENCE IMAGING OF SILICON WAFERS*, WPEC, Hawaii, 2006, in press
[6] T. Trupke et al., Proc. 19th EC-PVSEC, Paris, 2004, p. 758
[7] J. Isenberg, J. Dicker, W. Warta, J. Appl. Phys. **94**, 4122 (2003)
[8] J. Dicker, J. Isenberg, W. Warta, Proc. 17th EC-PVSEC, Munich, 2001, p. 1571
[9] D.A. Clugston and P.A. Basore, Proc. 26th IEEE PVSC, New York, 1997, p. 207
[10] J. Isenberg, PhD-thesis, Uni Konstanz (2003)
[11] T. Buaonassisi et al., Proc. 20th EC-PVSEC, Barcelona, 2005, p. 569